The Surface Energy Budget and Precipitation Efficiency of Convective Systems during TOGA COARE, GATE, SCSMEX and ARM: Cloud-Resolving Model Simulations

W.-K. Tao[1], C.-L. Shie[1,2], D. Johnson[1,2], and J. Simpson[1]

[1] *Laboratory for Atmospheres*
NASA/Goddard Space Flight Center
Greenbelt, MD 20771
USA

[2] *Goddard Earth Sciences and Technology Center*
University of Maryland, Baltimore County
Baltimore, MD

J. Atmos. Sci.

(August 20 2002)

Corresponding author address: Dr. Wei-Kuo Tao, Mesoscale Atmospheric Processes Branch, Code 912, NASA/GSFC, Greenbelt, MD 20771

email: tao@agnes.gsfc.nasa.gov

Surface Energy Budget and Precipitation Efficiency for Convective Systems during TOGA COARE, GATE, SCSMEX and ARM: Cloud-Resolving Model Simulations

W.-K Tao, C.-L. Shie, D. Johnson, and J. Simpson

Submitted to *Journal of Atmospheric Sciences*

Popular Summary

The Goddard Cumulus Ensemble (GCE) model (with 1-km grid resolution) is used to quantify the precipitation processes associated with active deep convective systems that developed over the South China Sea, West Pacific warm pool region, eastern Atlantic and Oklahoma. The GCE model results captured many of the observed precipitation characteristics in these convective systems because it used both a fine grid size and observed data from the well-planned field campaigns. For example, the temporal variation of the simulated area-averaged rainfall compares quite well to the sounding-estimated rainfall variation. The time- and domain-averaged temperature (heating/cooling) and water vapor (drying/moistening) budgets are also in good agreement with observations.

By examining the surface energy budgets, the model results indicated that the large-scale transports of heat (thermal energy) and moisture are the main energy sources for precipitation in the tropical cases. The effects of large-scale heat transport exceed that of large-scale moisture transport in the west Pacific warm pool region and eastern Atlantic region. For cloud systems that developed over the South China Sea, however, the effects of large-scale moisture transport predominate even though the cloud systems developed in a very moist environment. These results suggest that a delicate balance exist between cloud system response to local and large-scale (remote) processes.

For systems over the South China Sea and eastern Atlantic, net radiation (cooling) forces only about 20% or more of the precipitation. However, solar heating and infrared cooling are almost in balance for cloud systems over the West Pacific so that net radiation forcing is very small. This is due to the thick anvil clouds simulated in those systems. Net radiation (solar and infrared) and heat fluxes from the Earth's surface play a much more important role in the central USA.

The results showed that the precipitation efficiency (PE) varies from 32 to 45% for cloud systems in different geographic locations. No definite relationship between the PE and wind shear, or other characteristics of the large-scale environment, is found in these cloud ensemble model simulations. It is also found that there is no clear relationship between the PE and rainfall, the net condensation, or the large-scale transports of heat (thermal energy) and moisture.

The cloud data generated by the GCE model is used to improve satellite rainfall retrieval and the representation of cloud processes in large-scale models.

Abstract

A two-dimensional version of the Goddard Cumulus Ensemble (GCE) Model is used to simulate convective systems that developed in various geographic locations. Observed large-scale advective tendencies for potential temperature, water vapor mixing ratio, and horizontal momentum derived from field campaigns are used as the main forcing. By examining the surface energy budgets, the model results show that the two largest terms are net condensation (heating/drying) and imposed large-scale forcing (cooling/moistening) for tropical oceanic cases. These two terms are opposite in sign, however.

The contributions by net radiation and latent heat flux to the net condensation vary in these tropical cases, however. For cloud systems that developed over the South China Sea and eastern Atlantic, net radiation (cooling) accounts for about 20% or more of the net condensation. However, short-wave heating and long-wave cooling are in balance with each other for cloud systems over the West Pacific region such that the net radiation is very small. This is due to the thick anvil clouds simulated in the cloud systems over the Pacific region. Large-scale cooling exceeds large-scale moistening in the Pacific and Atlantic cases. For cloud systems over the South China Sea, however, there is more large-scale moistening than cooling even though the cloud systems developed in a very moist environment.

For three cloud systems that developed over a mid-latitude continent, the net radiation and sensible and latent heat fluxes play a much more important role. This means the accurate measurement of surface fluxes and radiation is crucial for simulating these mid-latitude cases.

The result showed that precipitation efficiency (PE) varies from 32 to 45% between cloud systems from different geographic locations. No definite relationship between the PE and wind shear, and the large-scale environment is found in these cloud ensemble model

simulations. It is also found that there is no clear relationship between the PE and rainfall, the net condensation, or the large-scale forcing.

1. Introduction

Cloud-resolving (or cumulus ensemble) models (CRMs) are one of the most important tools used to establish quantitative relationships between diabatic heating and rainfall. This is because latent heating is dominated by phase changes between water vapor and small, cloud-sized particles, which can not be directly detected. CRMs have sophistical microphysical processes that can explicitly simulate the conversion of cloud condensate into raindrops and various forms of precipitation ice. For this reason, CRMs were chosen as the primary approach to improve the representation of moist processes in global circulation and climate models [GEWEX Cloud System Study (GCSS) Science Plan 1994]. Progress in studying precipitating convective systems in GCSS is reported in Moncrieff *et al.* (1997).

The CRMs were extensively used to study tropical convection and its relation to the large-scale environment during the past two decades. Typically, the large-scale effects derived from observations are imposed into the models as the main forcing. When the imposed large-scale advective forcing cools and moistens the environment, the model responds by producing clouds through condensation and deposition. The fall out of large precipitation particles produces rainfall at the surface. The larger the advective forcing, the larger the microphysical response (rainfall) the model can produce (Soong and Tao 1980, Tao and Simpson 1984). On the other hand, the model will not produce any cloud nor rainfall when the imposed large-scale advective forcing heats and dries the atmosphere.

The CRMs, however, need to use cyclic lateral boundary conditions to ensure that there was no additional heat, moisture or momentum forcing inside the domain apart from the large-scale forcing. The CRMs also require a large horizontal domain to allow for the existence of an ensemble of clouds/cloud systems of different sizes in various stages of their lifecycles. The advantage of this CRM approach is that the modeled convection will be forced to almost the same (but not identical) intensity, thermodynamic budget and organization as the observations. This type of cloud-resolving modeling was used by many modeling studies for studying GATE, TOGA COARE, DOE/ARM, and SCSMEX[1] convective systems (Soong and Tao 1980, 1984, Tao and Soong 1986, Krueger 1988, Wu and Randall 1996, Xu *et al.* 1998, 1999, Grabowski *et al.* 1996, 1998, Das *et al.* 1999, Li *et al.* 1999, Donner *et al.* 1999, Xu *et al.* 2002, Johnson *et al.* 2002, Tao 2002, Tao *et al.* 2000, 2002a and others). The key developments in cloud ensemble modeling over the past two decades were listed in Table 1 in Tao (2002).

The Goddard Cumulus Ensemble (GCE) model is a cloud-resolving model. It has been used to simulate active convective events during GATE, TOGA COARE, ARM and SCSMEX. In this paper, the results from multi-day GCE model simulations will be used to calculate the surface energy budget. Then, the similarities and differences in surface energy budgets between these convective systems that developed in these different large-scale environments will be examined. In addition, precipitation efficiency associated with these different convcetive systems will be examined and compared.

2. Large-Scale Environmental Conditions

The most intense convection during TOGA COARE occurred in middle and late December 1992, prior to the peak of westerly wind bursts around 1 January 1993. Westerlies started to appear near the surface over the TOGA COARE Intensive Flux Array (IFA) in early December and gradually developed and intensified, although the middle and upper troposphere were still dominated by easterlies. Several major convective events occurred around 11-16 and 20-25 December 1992, mainly due to low-level large-scale convergence of easterlies and westerlies. However, the synoptic conditions were different for these two December events. Easterly flow

---

1 SCSMEX stands for South China Sea Monsoon experiment, GATE stands for Global Atmospheric Research Programme (GARP) Atlantic Experiment. TOGA-COARE stands for Tropical Ocean-Global Atmosphere Program - Coupled Ocean-Atmosphere Response Experiment. DOE/ARM stands for Department of Energy Atmospheric Radiation Measurement Program.

prevailed at low levels from near the date line westward to the IFA, and convection over the IFA arrived from the east with an easterly surge on 11-16 December. During 21-24 December, there was a greater contribution to heating from stratiform precipitation caused by the increased wind shear (Lin and Johnson 1996). There was less of a stratiform contribution for the December 11-16 convective episode. These two different periods, December 10-17, 1992 and December 19-27, 1992, have been simulated using the two-dimensional version of the GCE model (Das *et al.* 1999, Tao *et al.* 2000, and Johnson *et al.* 2002). The large-scale forcing used in the GCE model was derived form IFA sounding networks (Lin and Johnson 1996).

The cloud systems (non-squall clusters, a squall line, and scattered convection) for the period of 1-7 September 1974 phases III of the GATE have also been simulated using the GCE model (Li *et al.* 1999, Tao 2002). Sui and Yanai (1986) provided the GATE large-scale forcing for the GCE model. The same large-scale forcing was used in Grabowski *et al.* (1996). The large-scale environments associated with the organized cloud systems that occurred in TOGA COARE and GATE were quite different even though both are over tropical oceans. The large-scale advective forcing in temperature and water vapor as (see Fig. 1) well as the large-scale vertical velocity are stronger for TOGA COARE. The vertically integrated water vapor content (precipitable water) is much drier for GATE than TOGA COARE (Table 1). The mean CAPE is slightly smaller in GATE than in TOGA COARE.

The South China Sea Monsoon Experiment (SCSMEX) was conducted in May-June 1998 and one of its major objectives is to better understand the key physical processes for the onset and evolution of the summer monsoon over Southeast Asia and southern China (Lau *et al.* 2000). Two multi-day integrations using SCSMEX data (Johnson and Ciesielski 2002) were simulated using the GCE model (Tao *et al.* 2002a). The first one is prior to and during the monsoon onset period (May 18-26, 1998), and the second is after the onset of the monsoon (June 2–11, 1998). The mean large-scale forcing associated with these two cases is different

(Fig. 1). For example, the large-scale forcing in water vapor is much stronger in the lower and middle troposhere in the June case. In addition, the CAPE is larger in the June period than in the May one (Table 1). Note that the large-scale forcing in water vapor has more complex vertical structures (multi-peaks) in SCSMEX compared to those of GATE and TOGA COARE (single peaks located at low to middle altitude, see Fig. 1). The vertically integrated water vapor contents are very moist for the SCSMEX cases compared to the two TOGA COARE cases.

The ARM Summer 1997 Intensive Observing Period (IOP) at the Southern Great Plains (SGP) ARM Cloud and Radiation Testbed (CART) site in northern Oklahoma covers a 29-day period from 18 June to 17 July. Three sub-periods, 26-30 June, 7-12 July and 12-17 July 1997, are simulated using the GCE model[2]. One major difference between the ARM simulations and the SCSMEX, TOGA COARE and GATE simulations is that interactive cloud-radiation and air-sea processes are not allowed in the ARM runs. Radiative heating rate profiles based on the European Center for Medium-range Weather Forecasting (ECMWF) that are adjusted by the observed column radiative fluxes and observed surface turbulent (latent and sensible) heat fluxes from Energy Balance/Bowen Ratio (EBBR) measurements are imposed. As expected, the vertically integrated water vapor contents are very dry and the CAPE is larger in these mid-latitude continental ARM cases (Table 1). See Zhang and Lin (1997) and Xu *et al.* (2002) for more details on the ARM cases and their associated large-scale forcing.

3. The Goddard Cumulus Ensemble (GCE) Model

The model used in this study is the two-dimensional (2-D) version of the Goddard Cumulus Ensemble (GCE) model. The equations that govern cloud-scale motion (wind) are anelastic by filtering out sound waves. The subgrid-scale turbulence used in the GCE model is based on work by Klemp and Wilhelmson (1978) and modified by Soong and Ogura (1980) by including the effect of condensation on the generation of subgrid-scale kinetic energy. The cloud microphysics include a parameterized two-category liquid water scheme (cloud water and rain), and a parameterized Lin *et al.* (1983) or Rutledge and Hobbs (1984) three-category ice-phase scheme (cloud ice, snow and hail/graupel). Graupel is used in the SCSMEX, TOGA COARE and GATE simulation and hail is used for the ARM cases. Shortwave (solar) and longwave (infrared) radiation parameterizations are also included in the model (Tao *et al.* 1996). The TOGA-COARE bulk flux algorithm (Fairall *et al.* 1995) is linked to the GCE model for calculating the surface fluxes (Wang *et al.* 1996). All scalar variables (potential temperature, mixing ratio of water vapor, turbulence coefficients, and all five hydrometeor classes) use forward time differencing and a positive definite advection scheme with a non-oscillatory option (Smolarkiewicz and Grabowski, 1990). The dynamic variables, u, v and w, use a second-order accurate advection scheme and a leapfrog time integration (kinetic energy semi-conserving method). Details of the GCE model description and improvements can be found in Tao and Simpson (1993) and Tao *et al.* (2002b).

For the present study, a stretched vertical coordinate with 41 levels is used. The model has finer resolution (about 80 meters) in the boundary layer and coarser resolution (about 1000 meters) in the upper levels. The grid spacing in the horizontal plane is 1000 meters with 512 grid points. The time step is 6 s for the ARM cases and 7.5 s for the SCSMEX, TOGA COARE and GATE cases.

4. Results

4.1 Energy Budget

Horizontal and vertical integration of the equations for temperature, water vapor (q_v), and moist static energy h ($h = CpT + L_v q_v + gz$) over the entire model domain yields

---

[2] These three period have also been used by the GEWEX Cloud System Study (GCSS) working group 4 (WG4) model intercomparison project for CRMs and Single Column Models (SCMs).

$$C_p < \frac{\partial \overline{T}}{\partial t} > = < L_v(\bar{c} - \bar{e}) + L_f(\bar{f} - \overline{m}) + L_s(\bar{d} - \bar{s}) > - C_p < \frac{\partial \overline{\theta}}{\partial t} >_{L.S} + \overline{Q}_R + C_p \overline{H}_s \quad (1)$$

$$L_v < \frac{\partial \overline{q}_v}{\partial t} > = - < L_v(\bar{c} - \bar{e}) + L_s(\bar{d} - \bar{s}) > - L_v < \frac{\partial \overline{q}_v}{\partial t} >_{L.S} + L_v \overline{E}_o \quad (2)$$

$$< \frac{\partial \overline{h}}{\partial t} > = < L_f(\bar{f} - \overline{m}) + (L_s - L_v)(\bar{d} - \bar{s}) > - (C_p < \frac{\partial \overline{\theta}}{\partial t} >_{L.S} + L_v < \frac{\partial \overline{q}_v}{\partial t} >_{L.S}) + \overline{Q}_R + C_p \overline{H}_s + L_v \overline{E}_o \quad (3)$$

where $- < \frac{\partial \overline{\theta}}{\partial t} >_{L.S}$ and $- < \frac{\partial \overline{q}_v}{\partial t} >_{L.S}$ are the large-scale advective cooling and moistening; E_O and H_S are the latent and sensible heat fluxes from the ocean surface. The physical processes responsible for the precipitation processes in each case can be quantified by examining the budget. In addition, the similarities and differences in terms of large-scale forcing, surface fluxes and radiation upon precipitation (net condensation) between different active convective events that developed in different geographic locations can be identified.

Tables 2 and 3 list the temperature and water vapor budgets for the SCSMEX, TOGA COARE, GATE and ARM cases. In the tropical oceanic cases (SCSMEX, TOGA COARE and GATE), the largest two terms in the temperature and water vapor budget are net condensation (heating/drying) and imposed large-scale forcing (cooling/moistening). These two terms are opposite in sign, however. Soong and Tao (1980) performed experiments with different magnitudes of large-scale forcing and found that the larger the large-scale forcing (cooling/moistening), the larger the net condensation (heating/drying). They suggested that the effect of cloud microphysics is simply a response to the "imposed large-scale forcing in temperature and water vapor". The sensible heat flux is at least one order of magnitude smaller than net condensation and large-scale forcing in these tropical oceanic cases.

The contributions by net radiation (shortwave heating and longwave cooling) and latent heat flux on the net condensation vary in these tropical cases, however. For the SCSMEX and

GATE cases, the net radiation (cooling) accounts for about 20% or more of the net condensation. This result suggests that net radiation plays an important role in the precipitation processes for the SCSMEX and GATE cases. Net radiation is very small and does not contribute to the total net condensation (precipitation processes) for the TOGA COARE cases. This is because thick anvil clouds are simulated in the TOGA COARE cases. However, the radiation process still plays an important role in the diurnal variability of rainfall for the TOGA COARE convective systems (i.e., Sui *et al.* 1997, Johnson *et al.* 2002 and others).

Latent heat fluxes are important for precipitation processes in the tropical convective systems except for one of the SCSMEX cases. Latent heat flux is an order of magnitude smaller than both large-scale forcing and net condensation in the water vapor budget for the June SCSMEX case. This is because the large-scale advective forcing in water vapor was very large in the lower troposphere and generated a moist boundary layer (Fig. 1). This reduced the contribution from latent heat fluxes from the ocean for this case.

Net radiation and sensible and latent heat fluxes play a much more important role in the three ARM cases than in the tropical cases (Tables 2 and 3). Latent heat fluxes are much larger than the large-scale forcing in the water vapor budget for the two July cases (relatively weak events compared to other cases). They contribute 76% and 90% of the net condensation for the two July cases, respectively. They are the main source of moisture for condensation. Net radiation can be as large as the large-scale temperature forcing in the ARM cases (Table 2). This means the accurate measurement of surface fluxes and radiation is crucial for simulating the ARM cases.

It is well known that temperature and water vapor are closely related. Evaporative cooling/condensational heating is a source/sink for the water vapor field. On the other hand, latent heat flux from the ocean surface can provide water vapor for condensation heating. The moist static energy budget (Table 4) can provide some additional information on the physical processes for these active convective events. The net condensation in the moist static energy budget are melting (cooling), freezing (heating), and the product of the latent heat of fusion and the net deposition (deposition subtract sublimation)[3]. These microphysical processes are usually the smallest terms in the moist static energy budget.

Large-scale forcing and surface latent heat fluxes are largest in the TOGA COARE cases. They are approximately an order of magnitude larger than the other processes in the moist static energy budget. Interestingly, the large-scale forcing in the moist static energy budget is negative (large-scale cooling exceeds large-scale moistening) for the TOGA COARE and GATE cases. For SCSMEX, however, there is more large-scale moistening than cooling. This suggests that the imposed large-scale advective forcing in water vapor is important for convective processes in the SCSMEX cases even though the SCSMEX convective systems developed in a very moist environment (Table 1). The net radiation is quite important in the SCSMEX, GATE and ARM cases. For some cases, it is the largest term in the moist static energy budget.

Note that the net condensation is very small in both the TOGA COARE cases and in two of the ARM cases. This suggests that there is a balance between the melting and freezing, and the deposition and sublimation in these cases. A positive (negative) value in net condensation in the moist static energy indicates the sum of freezing and deposition is larger (smaller) than the sum of melting and sublimation.

The surface (sensible and latent heat) fluxes are largest in the ARM cases. However, the surface budget for the June ARM case is different from the two July cases. First, the large-scale water vapor forcing is important and contributes about 65% of the net condensation in the

---

[3] This term is usually positive (i.e., releasing heat in the model simulation).

June case (Table 3). Second, the large-scale water vapor forcing is stronger than the large-scale temperature forcing in the June case (Table 4).

5. Precipitation Efficiency

The total precipitation efficiency (PE) in the simulations can be defined as the ratio of the total rainfall to the total condensation (condensation onto water plus deposition onto ice for all hydrometeor species). A similar definition of precipitation efficiency was adopted in the three-dimensional modeling study of Weisman and Klemp (1982), in which precipitation efficiencies varied from 11 to 49 percent over the 2-h duration of their simulations. Ferrier *et al.* (1996) investigated the precipitation efficiency of convective systems under widely varying large-scale conditions using the GCE model. Their results indicated that the vertical orientation of the updrafts, which is controlled by the vertical wind shear, and the ambient moisture content are important in determining precipitation efficiency. However, these modeling studies only examined the PE associated with individual clouds or cloud systems, not ensembles of clouds/cloud systems.

The total PE ranges from 32% to 45% in the GCE-simulated SCSMEX, TOGA COARE, GATE and ARM cases (Table 5). The two SCSMEX cases have very similar PEs (45.4 and 45.3%) and are the largest among all the simulations. This result suggests that the larger vertical u-wind shear in the June SCSMEX case does not produce a larger precipitation efficiency. However, one of the TOGA COARE case (December 19-26) has a larger PE as well as stronger wind shear than the other TOGA COARE case (December 10-17). It may be expected that the ARM (midlatitude and continental) and GATE cases would have lower PEs because they developed under drier environments. One of the ARM July cases has the smallest PE (32%), but the GATE and the June ARM cases have relatively large PEs, 44.5% and 40.1%, respectively. No definite relationship between the PE and wind shear and/or the large-scale environment is found in these cloud ensemble model simulations. It is also found that there is no clear relationship between the PE and rainfall, the net condensation, or the large-scale forcing (Tables 2, 3, 4 and 5). However, the model results show that the two SCSMEX cases and the GATE case have large, positive net condensation in the moist static energy budget, and they all have larger PEs. One of the ARM June cases and one of the TOGA COARE cases have negative net condensation as well as small PE. A positive net condensation in the moist static energy budget indicates that there is net melting (melting subtract freezing) and/or net deposition (deposition subtract sublimation).

The rainfall amount simulated by the GCE model and estimated by soundings is in excellent agreement (within 0.5%) with each other for both TOGA COARE cases (i.e., Johnson *et al.* 2002). The model underestimates the rainfall by 10%, 17% and 20%, respectively, for the GATE and SCSMEX May and June cases compared to that calculated based on soundings (Das *et al.* 1999, Tao *et al.* 2002a). For the ARM cases, however, the GCE model underestimates rainfall by about 10% in the June case and overestimate rainfall by 16% and 10%, respectively, for the two July cases (Wu *et al.* 2002)[4]. All of these cases are forced by a prescribed large-scale advective forcing determined from soundings. The radiation and surface fluxes can be influenced by clouds simulated by the models and may cause the rainfall differences between the model and the sounding estimates. For the ARM cases, the radiation and surface fluxes are prescribed, but not for the SCSMEX, GATE and TOGA COARE cases. Based on the moist static energy budget, the GCE can underestimate the rainfall when a positive large-scale forcing is imposed/prescribed (except for the GATE case). This result may imply that the GCE model could underestimate the rainfall (when compared to sounding estimates) when the large-scale advective water vapor forcing exceeds the large-scale temperature forcing. More thorough cloud ensemble modeling studies will be needed to generalize this relationship as well as the relationship between PE and net condensation in the moist static energy budget.

[4] Similar errors have been found with other cloud-resolving models in simulating ARM and TOGA COARE cases.

5. Summary and Conclusions

The two-dimensional version of the GCE model has been used to simulate two SCSMEX [May 18-26 and June 2-11, 1998], two TOGA COARE (December 10-17 and 19-26 1992), one GATE (September 1-2 1974) and three ARM convective active periods (June 26-30, July 7-12 and July 12-17, 1997), and those results are compared with each other. Observed large-scale advective tendencies (or forcing) of potential temperature, water vapor mixing ratio, and horizontal momentum (Sui and Yanai 1986, Lin and Johnson 1996, Zhang and Lin 1997, and Johnson and Ciesielski 2002) are used as the main forcing in governing the GCE model in a semi-prognostic manner (Soong and Tao1980, Tao and Soong 1986, and many others). The surface energy budget and precipitation efficiency were examined by using the model results.

The major results can be summarized as follows:

- Large-scale advective forcing in temperature and water vapor are the major energy sources for net condensation in the tropical oceanic cases. The large-scale cooling exceeds large-scale moistening for the TOGA COARE and GATE cases. For SCSMEX, however, there is more large-scale moistening than cooling. Interestingly, the vertically integrated water vapor contents are very moist for the SCSMEX cases compared to the TOGA COARE and GATE cases.

- The net radiation and the sensible and latent heat fluxes play a much more important role in the three ARM cases. Latent heat fluxes contribute 76% and 90% of the net condensation for the two ARM July cases.

- The contributions by net radiation and latent heat flux on the net condensation vary in the tropical cases, however. For the SCSMEX and GATE cases, the net radiation (cooling) accounts for about 20% or more of the net condensation. Net radiation is very small and does not contribute to the total net condensation (precipitation processes) for the TOGA COARE cases. This is because thick anvil clouds are simulated in the TOGA COARE cases. However, the radiation process still plays an important role in the diurnal variability of rainfall for the TOGA COARE convective systems.

- The model results showed that the precipitation efficiency (PE) varies, from 32 to 45%, between the cloud systems from different geographic locations. Similar ranges of PE were also found by Ferrier *et al.* (1996). But, no definite relationship between the PE and wind shear and/or the large-scale environment is found in these cloud ensemble model simulations. This conclusion is different from the isolated cloud system simulations by Ferrier *et al.* (1996). It is also found that there is no clear relationship between the PE and rainfall, the net condensation, or the large-scale forcing. Nevertheless, the results suggest that cases with large, positive net condensation in the moist static energy budget tend to have a large PE.

- The model results suggest that the GCE can underestimate the rainfall when a positive large-scale forcing is imposed/prescribed (except for the GATE case). More thorough cloud ensemble modeling studies will be needed to generalize these relationships.

Real clouds and cloud systems are three-dimensional. Because of the limitations of computer resources, however, most cloud ensemble models (CEMs) or CRMs today are still two-dimensional. Few 3-D CEMs (e.g., Tao and Soong 1986; Tao *et al.* 1987; Lipps and Hemler 1986) have been used to study the response of clouds to large-scale forcing. In these 3-D simulations, the model domain was small and integration times were between 3 and 6 hours. Only recently, 3-D experiments were performed for multi-day periods for tropical cloud systems with large horizontal domains (Grabowski *et al.* 1998, Donner *et al.* 1999 and Tao 2002). Grabowski *et al.* (1998) and Tao, (2002) found that that cloud statistics as well as surface precipitation and latent heating profiles are very similar between the multi-day 2-D and 3-D simulations for GATE and TOGA COARE cases. The reason for the strong similarity between the 2-D and 3-D CRM simulations is that the same observed (time-varying) large-scale advective tendencies of potential temperature, water vapor mixing ratio, and horizontal momentum were used as the main forcing in both the 2-D and 3-D models. We are in the process of using the 3-D GCE model to simulate these ARM and SCSMEX and other cases and will report our results in a publication in the near future.

5. Acknowledgements

This work is mainly supported by the NASA Headquarters Atmospheric Dynamics and Thermodynamics Program and the NASA Tropical Rainfall Measuring Mission (TRMM). The authors are grateful to Dr. R. Kakar at NASA headquarters for his support of this research. The authors thank Mr. S. Lang for reading the manuscript.

Acknowledgment is also made to the NASA/Goddard Space Flight Center for computer time used in this research.

6. References

Cotton, W. R. and G. J. Tripoli, 1978: Cumulus convection in shear flow - three-dimensional numerical experiments. *J. Atmos. Sci.*, 35, 1053-1521.

Das, S., D. Johnson and W.-K. Tao, 1999: Single-column and cloud ensemble model simulations of TOGA COARE convective systems, *J. Meteor. Soc. Japan*, 77, 803-826.

Donner, L. J., C. J. Seman abd R. S. Hemler, 1999: Three-dimensional cloud-system modeling of GATE convection, *J. Atmos. Sci.*, 56, 1885-1912.

Ferrier, B. S., J. Simpson and W.-K. Tao, 1996: Factors responsible for different precipitation efficiencies between midlatitude and tropical squall simulations, *Mon. Wea. Rev.*, 124, 2100-2125.

Fairall, C., E.F. Bradley, D.P. Rogers, J.B. Edson, and G. S. Young, 1996: Bulk parameterization of air-sea fluxes for TOGA COARE. *J. Geophy. Res.*, 101, 3747-3764.

Grabowski, W. W., X. Wu, and M. W. Moncrieff, 1996: Cloud-resolving modeling of cloud systems during Phase III of GATE. Part II: Two-dimensional experiments. *J. Atmos. Sci.*, 53, 3684- 3709.

Grabowski, W. W., X. Wu, M. W. Moncrieff, and W. D. Hall, 1998: Cloud-resolving modeling of cloud systems during Phase III of GATE. Part II: Effects of resolution and the third spatial dimension. *J. Atmos. Sci.*, 55, 3264- 3282.

Johnson, R. H., and P. E. Ciesielski, 2002: Characteristics of the 1998 summer monsoon onset over the Northern South China Sea. *J. Metro. Soc. Japan*, (submitted).

Johnson, D., W.-K. Tao, J. Simpson, and C.-H. Sui, 2002: A study of the response of deep tropical clouds to large-scale processes, Part I: Model set-up strategy and comparison with observation, *J. Atmos. Sci.*. (in press).

Klemp, J. B., and R. Wilhelmson, 1978: The simulation of three-dimensional convective storm dynamics. *J. Atmos. Sci.*, 35, 1070-1096.

Krueger, S. K., 1988: Numerical simulation of tropical cumulus clouds and their interaction with the subcloud layer. *J. Atmos. Sci.*, 45, 2221-2250.

Lau, K. M., Y. Ding, J.-T. Wang, R. Johnson, T. Keenan, R. Cifelli, J. Geriach, O. Thiele, T. Rickenbach, S.-C. Tsay, and P.-H. Lin, 2000: A report of the field operations and early results of the South China Sea Monsoon experiment (SCSMEX). *Bull. Amer. Meteor. Soc.*, 81, 1261-1270.

Li, X., C.-H. Sui, K.-M. Lau and M.-D. Chou, 1999: Large-scale forcing and cloud-radiation interaction in the tropical deep convective regime. *J. Atmos. Sci.*, **56**, 3028-3042.

Lin, Y.-L., R. D. Farley and H. D. Orville, 1983: Bulk parameterization of the snow field in a cloud model. *J. Clim. Appl. Meteor.*, 22, 1065-1092.

Lin, X., and R. H. Johnson, 1996: Heating, moistening and rainfall over the western Pacific during TOGA COARE. *J. Atmos. Sci.*, 53, 3367-3383.

Moncrieff, M. W., S. K. Krueger, D. Gregory, J.-L. Redelsperger and W.-K. Tao, 1997: GEWEX Cloud System Study (GCSS) Working Group 4: Precipitating convective cloud systems. *Bull. Amer. Meteor. Soc.*, **78**, 831-845.

Redelsperger, J. L., P. R. A. Brown, F. Guichard, C. Hoff, M. Kawasima, S. Lang, Th. Montmerle, K. Nakamura, K. Saito, C. Seman, W.-K. Tao and L. J. Donner, 2000: A

GCSS model intercomparison for a tropical squall line observed during TOGA-COARE. Part 1: Cloud-Resolving Models. *Q. J. R. Met. Soc.*, 126, 823-864.

Rutledge, S.A., and P.V. Hobbs, 1984: The mesoscale and microscale structure and organization of clouds and precipitation in midlatitude clouds. Part XII: A diagnostic modeling study of precipitation development in narrow cold frontal rainbands. *J. Atmos. Sci.*, 41, 2949-2972.

Smolarkiewicz, P. K., and W. W. Grabowski, 1990: The multidimensional positive advection transport algorithm: Nonoscillatory option. *J. Comput. Phys.*, 86, 355-375.

Soong, S.-T., and Y. Ogura, 1980: Response of tradewind cumuli to large-scale processes. *J. Atmos. Sci.*, 37, 2035-2050.

Soong, S.-T., and W.-K. Tao, 1980: Response of deep tropical clouds to mesoscale processes. *J. Atmos. Sci.*, 37, 2016-2036.

Sui, C,-H., and M. Yanai, 1986: Cumulus ensemble effects on the large-scale vorticity and momentum fields of GATE. Part I: Observational evidence. *J. Atmos. Sci.*, **43**, 1618-1642.

Sui, C.-H., and K.-M. Lau and X. Li, 1998: Convective-radiative interaction in simulated diurnal variations of tropical cumulus ensemble. *J. Atmos. Sci.*, **55**, 2345-2357.

Tao, W.-K., and J. Simpson, 1984: Cloud interactions and merging: Numerical simulations. *J. Atmos. Sci.,* 41, 2901-2917.

Tao, W.-K., and S.-T. Soong, 1986: A study of the response of deep tropical clouds to mesoscale processes: Three-dimensional numerical experiments. *J. Atmos. Sci.*, 43, 2653-2676.

Tao, W.-K., J. Simpson, and S.-T. Soong, 1987: Statistical properties of a cloud ensemble: A numerical study. *J. Atmos. Sci.*, 44, 3175-3187.

Tao, W.-K., and J. Simpson, 1989: Modeling study of a tropical squall-type convective line. *J. Atmos. Sci.*, 46, 177-202.

Tao, W.-K., and J. Simpson, 1993: The Goddard Cumulus Ensemble Model. Part I: Model description. *Terrestrial, Atmospheric and Oceanic Sciences*, 4, 19-54.

Tao, W.-K., J. Scala, B. Ferrier, and J. Simpson, 1995: The effects of melting processes on the development of a tropical and a mid-latitudes squall line. *J. Atmos. Sci.*, 52, 1934-1948.

Tao, W.-K., J. Simpson, S. Lang, C.-H. Sui, B. Ferrier, and M.-D. Chou, 1996: Mechanisms of cloud-radiation interaction in the tropics and midlatitudes. *J. Atmos. Sci* . 53, 2624-2651.

Tao, W.-K., S. Lang, J. Simpson, W. S. Olson, D. Johnson, B. Ferrier, C. Kummerow and R. Adler, 2000: Vertical profiles of latent heat release and their retrieval in TOGA COARE convective systems using a cloud resolving model, SSM/I and radar data, *J. Meteor. Soc. Japan,* 78, 333-355.

Tao, W.-K., 2002: Goddard Cumulus Ensemble (GCE) model: Application for understanding precipitation processes, *AMS Meteorological Monographs - Cloud Systems, Hurricanes and TRMM.* (in press).

Tao, W.-K., C.-L. Shie, D. Johnson, R. Johnson, S. Braun, J. Simpson, and P. E. Ciesielski, 2002a: Convective Systems over South China Sea: Cloud-Resolving Model Simulations, *J. Atmos. Sci.* (submitted).

Tao, W.-K., J. Simpson, D. Baker, S. Braun, M.-D. Chou, D. Johnson, B. Ferrier, A. Khain, S. Lang, B. Lynn, C.-L. Shie, D. Starr, C.-H. Sui, Y. Wang and P. Wetzel, 2002b: Microphysics, Radiation and Surface Processes in a Non-hydrostatic Model. *Meteorology and Atmospheric Physics* (in press).

Wang, Y., W.-K. Tao and J. Simpson, 1996: The impact of ocean surface fluxes on a TOGA COARE cloud system *Mon. Wea. Rev.,* 124, 2753-2763.

Weisman, M. L., J. B. Klemp, and R. Rotunno, 1988: Structure and evolution of numerically simulated squall lines. *J. Atmos. Sci.*, 45, 1990-2013.

Wilhelmson, R. B., and J. B. Klemp, 1978: A numerical study of storm splitting that leads to long-lived storms. *J. Atmos. Sci.*, 35, 1975-1986.

Wu, X., W. W. Grabowski and M. W. Moncrieff, 1998: Long-term behavior of cloud systems in TOGA COARE and their interactions with radiative and surface processes. Part I: Two-dimensional modeling study. *J. Atmos. Sci.*, 55, 2693-2714.

Wu, X., W. W. Grabowski and M. W. Moncrieff, 1999: Long-term behavior of cloud systems in TOGA COARE and their interactions with radiative and surface processes. Part II: Effects of the ice microphysics on cloud-radiation interaction. *J. Atmos. Sci.*, 56, 3177-3195.

Xu, K.-M., 1995: Partitioning mass, heat, and moisture budgets of explicit simulated cumulus ensembles into convective and stratiform components. *J. Atmos. Sci.*, 52, 551-573.

Xu, K.-M., R. T. Cederwall, L. J. Donner, F. Guichard, W. W. Grabowski, D. E. Johnson, M. Khairoutdinov, S. K. Krueger, J. C. Petch, D. A. Randall, C. J. Seman, W.-K. Tao, S. Xie, J.

Jio and M.-H. Zhang, 2002: Iintercomparison of cloud-resolving models with the ARM Summer 1997 IOP data *Q. J. R. Met. Soc.,* 128, 593-624.

Zhang, M.-H., and J. L. Lin, 1997: Constrained variational analysis of sounding data based on column-integrated budgets of mass, moisture and momentum: Approach and application to ARM measurements. *J. Atmos. Sci.,* **54**, 1503-1524.

Zipser, E. J. and M. A. LeMone, 1980: Cumulonimbus vertical velocity events in GATE. Part II: Synthesis and model core structure. *J. Atmos. Sci.*, 37, 2458-2469.

Figure Captions

Fig. 1 Time-averaged large-scale advective forcing in **(a)** temperature and **(b)** water vapor. The solid line is the SCSMEX 18-26 May 1998 period and the dashed line the 2-11 June 1998 period. **(c)** and **(d)** are the same as (a) and (b) except for the TOGA COARE (solid line is December 10-17 and the dashed line December 19-26 1992) and GATE (long-dashed line is September 1-7 1974) cases. **(e)** and **(f)** are the same as (a) and (b) except for the three ARM cases (solid line is 26-30 June, dashed line 7-12 July and long dashed line 12-17 July 1997).

Fig. 2 Time-averaged large-scale **(a)** w-wind for the two SCSMEX cases. The solid line is for the 18-26 May 1998 period, and the dashed line is for the 2-11 June period. **(b)** is the same as (a) except for the TOGA COARE (solid line is December 10-17 and dashed line December 19-26 1992) and GATE (long-dashed line is September 1-7 1974) cases. **(c)** is the same as (a) except for the three ARM cases (solid line is 26-30 June, dashed line 7-12 July and long dashed line 12-17 July 1997).

Fig. 3 Time averaged temperature and water vapor mixing ratio biases for **(a)** SCSMEX, **(b)** TOGA COARE, **(c)** GATE and ARM A, and **(d)** ARM B and ARM C cases.

TABLES

Table 1 Initial environmental conditions expressed in terms of CAPE (Convective Available Potential Energy) and precipitable water for the SCSMEX (18-26 May and 2-11 June 1998), TOGA COARE (10-17 and 19-26 December 1992), GATE (September 1-7, 1974) and ARM (June 26-30, July 7-12 and July 12-17, 1997) cases.

Table 2 Temperature budgets for the SCSMEX, TOGA COARE, GATE and ARM cases. Net condensation is the sum of condensation, deposition, evaporation, sublimation, freezing and melting of cloud. Large-scale forcing is the imposed large-scale advective effect on temperature, and d(T) is the local time change of temperature. Long wave cooling, short wave heating and their net radiative processes are shown in Q_R. Units are in C day^{-1}.

Table 3 Same as in Table 2 except for the water budgets. Net condensation is the sum of condensation, deposition, evaporation and sublimation of cloud. Large-scale forcing is the imposed large-scale advective effect on water vapor, and d(q_v) is the local time change of water vapor. Units are in mm day^{-1}.

Table 4 Same as Table 3 except for the moist static energy budget. Units are W m^{-2}. Note that a C day^{-1} cooling or warming in the local change term over the whole troposphere can lead to about 92 W m^{-2} in the temperature budget. Note that a one g/kg in the local time change over the whole troposphere can lead to about 280 W m^{-2} in the water vapor budget.

Table 5 Precipitation efficiency (PE in %), domain-averaged surface rainfall amounts (in mm day^{-1}) and total net condensation (condensation plus deposition, in mm day^{-1}) for the SCSMEX, TOGA COARE, GATE and ARM cases.

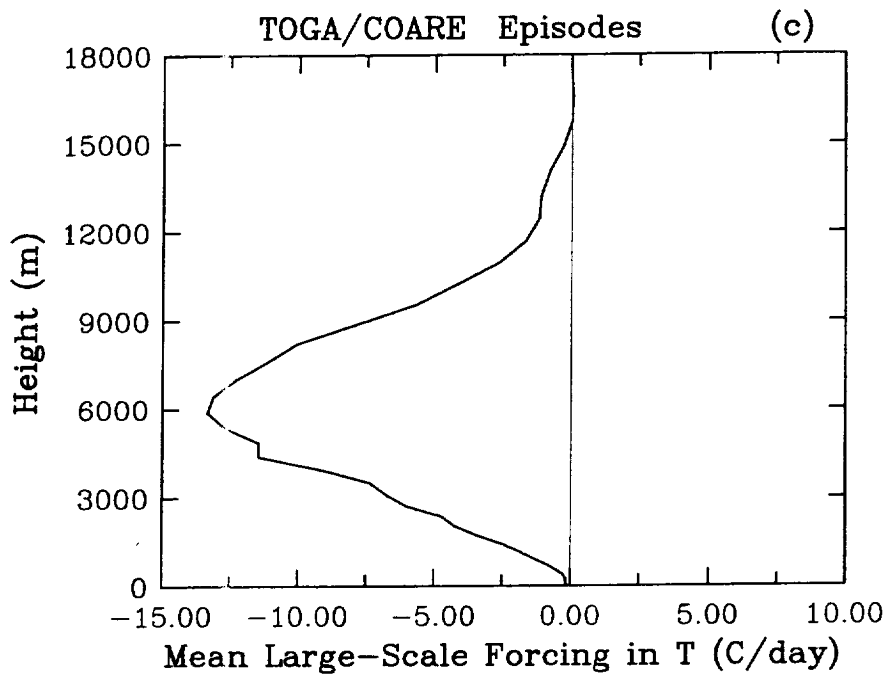
TOGA/COARE Episodes
(c)
18000
15000
12000
9000
6000
3000
0
Height (m)
−15.00
−10.00
−5.00
0.00
5.00
10.00
Mean Large−Scale Forcing in T (C/day)

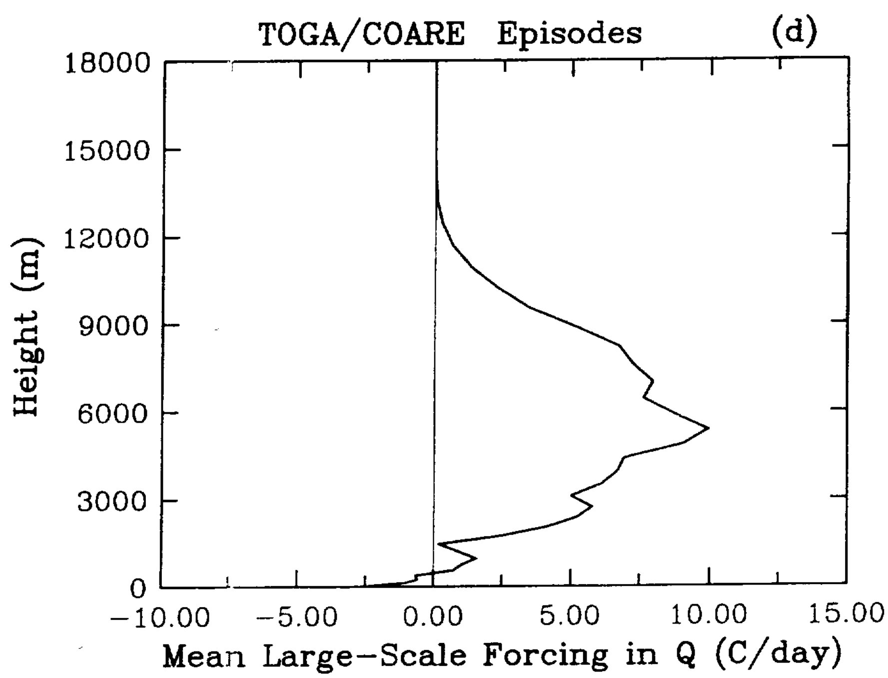
TOGA/COARE Episodes
(d)
18000
15000
12000
9000
6000
3000
0
Height (m)
−10.00
−5.00
0.00
5.00
10.00
15.00
Mean Large−Scale Forcing in Q (C/day)

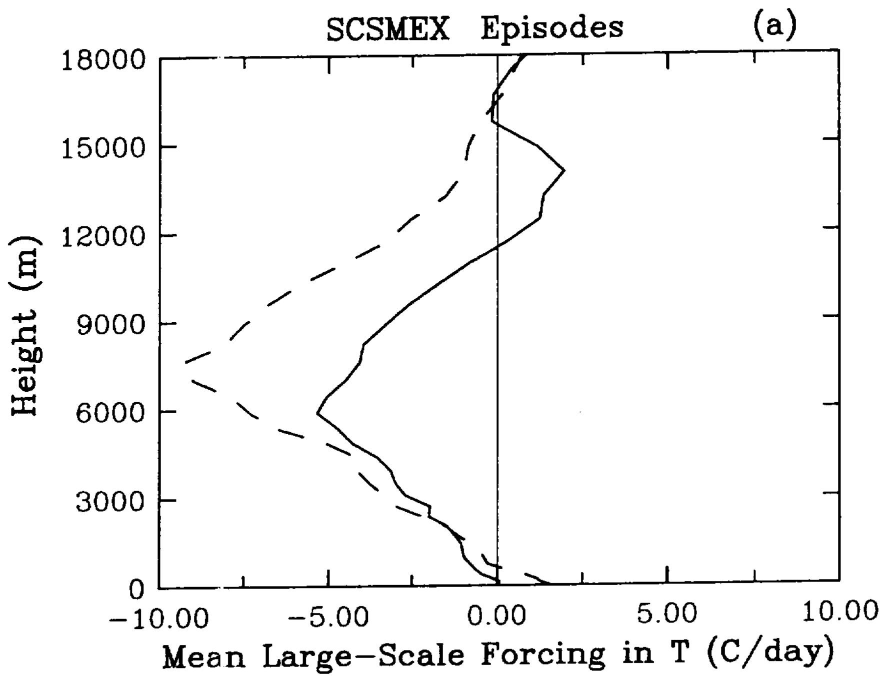
SCSMEX Episodes
(a)
Height (m)
18000
15000
12000
9000
6000
3000
0
−10.00
−5.00
0.00
5.00
10.00
Mean Large−Scale Forcing in T (C/day)

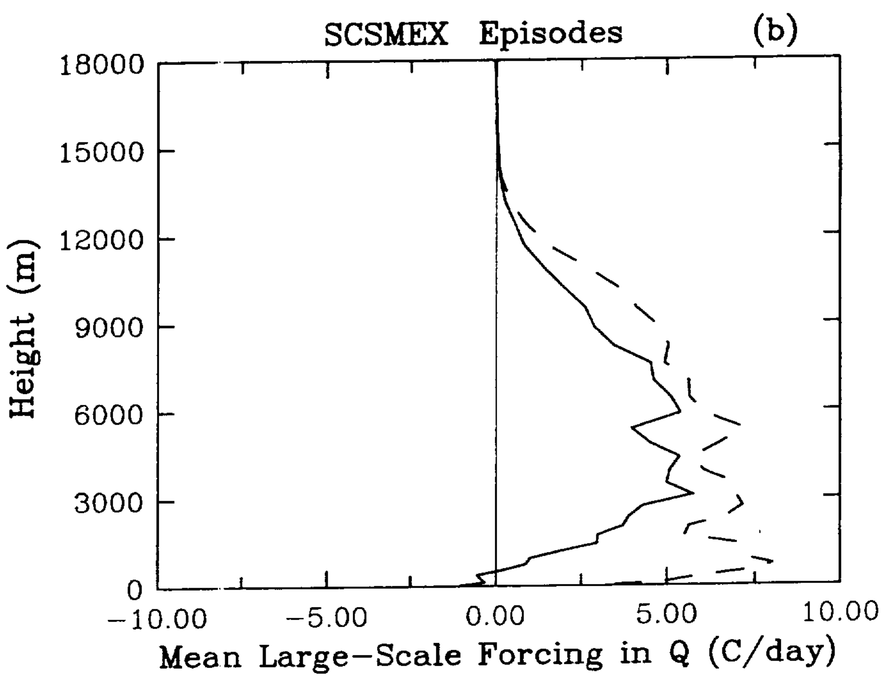
SCSMEX Episodes
(b)
Height (m)
18000
15000
12000
9000
6000
3000
0
−10.00
−5.00
0.00
5.00
10.00
Mean Large−Scale Forcing in Q (C/day)

Table 1

	CAPE m^2s^{-2}	Precipitable Water ($g\ cm^{-2}$)
SCSMEX (May18-26 1998)	825	62.53
SCSMEX (June 2–11 1998)	1324	62.34
TOGA COARE (December 19-26 1992)	898	54.64
TOGA COARE (December 10-17 1992)	1238	56.48
GATE (December 1-7 1974)	736	47.61
ARM (June 26-30 1997)	1954	37.76
ARM (July 7-12 1997)	1761	37.56
ARM (July 12-17 1997)	2806	36.80

Table 2

	dT/dt	Net Condensation	Large-scale Forcing	Net QR=SW-LW	Sensible Heat Fluxes
SCSMEX (May18-26 1998)	-0.12	2.83	-2.03	-0.95	0.03
SCSMEX (June 2–11 1998)	0.26	4.17	-2.88	-1.04	0.01
TOGA COARE (December 19-26 1992)	-0.29	5.06	-5.55	0.03	0.17
TOGA COARE (December 10-17 1992)	-0.28	4.33	-4.61	-0.11	0.11
GATE (December 1-7 1974)	-0.20	3.13	-2.67	-0.68	0.02
ARM (June 26-30 1997)	0.83	2.16	-1.01	-0.63	0.31
ARM (July 7-12 1997)	0.67	1.37	-0.41	-0.51	0.22
ARM (July 12-17 1997)	-0.16	1.28	-1.05	-0.66	0.27

Table 3

	d(Qv) /dt	Net Condensation	Large-scale Forcing	Latent Heat Fluxes
SCSMEX (May18-26 1998)	-0.15	-11.23	9.81	1.27
SCSMEX (June 2–11 1998)	1.12	-16.45	16.84	0.73
TOGA COARE (December 19-26 1992)	0.57	-20.15	15.03	5.69
TOGA COARE (December 10-17 1992)	-0.80	-17.31	13.47	3.04
GATE (December 1-7 1974)	-0.33	-12.30	9.90	2.07
ARM (June 26-30 1997)	1.24	-8.13	5.29	4.08
ARM (July 7-12 1997)	-0.02	-5.07	1.19	3.86
ARM (July 12-17 1997)	0.31	-4.83	0.80	4.34

Table 4

	D(CpT+ LvQv)	Net Condensation	Large-scale Forcing	Net Q_R	Sensible Heat Fluxes	Latent Heat Fluxes
SCSMEX (May18-26 1998)	-18.0	2.84	48.8	-110.7	4.2	36.85
SCSMEX (June 2–11 1998)	62.4	3.55	156.6	-119.9	1.07	21.11
TOGA COARE (December 19-26 1992)	-16.71	0.49	-204.96	3.34	19.76	164.66
TOGA COARE (December 10-17 1992)	-58.20	-0.98	-142.57	-12.75	29.86	87.91
GATE (December 1-7 1974)	-32.27	4.48	-21.14	-77.69	2.35	59.73
ARM (June 26-30 1997)	126.35	0.75	42.91	-68.93	33.62	118.00
ARM (July 7-12 1997)	72.24	2.14	-10.54	-54.96	23.85	111.75
ARM (July 12-17 1997)	-8.27	-0.78	-90.75	-72.19	29.74	125.71

Table 5

	Precipitation Efficiency (PE)	Rainfall (mm/day)	Condensation (mm/day)
SCSMEX (May 18-26 1998)	45.4	11.14	24.56
SCSMEX (June 2–11 1998)	45.3	16.46	36.31
TOGA COARE (December 19-26 1992)	41.6	20.15	48.39
TOGA COARE (December 10-17 1992)	37.5	17.81	47.52
GATE (December 1-7 1974)	44.5	12.31	27.67
ARM (June 26-30 1997)	40.1	7.51	18.72
ARM (July 7-12 1997)	39.9	4.68	11.74
ARM (July 12-17 1997)	32.1	4.29	13.37